

## Article

# Effect of the Particle Size Composition and Dry Density on the Water Retention Characteristics of Remolded Loess

Xin-Qing Wang <sup>1,2</sup>, Xiao-Chao Zhang <sup>1,\*</sup>, Xiang-Jun Pei <sup>1,\*</sup> and Guo-Feng Ren <sup>3</sup>

- <sup>1</sup> State Key Laboratory of Geohazard Prevention and Geoenvironment Protection, Chengdu University of Technology, Chengdu 610059, China; 2017010078@stu.cdut.edu.cn
- <sup>2</sup> Department of Architecture and Civil Engineering, Sichuan Vocational and Technical College of Communications, Chengdu 611130, China
- <sup>3</sup> Sichuan Water Resources and Hydroelectric Investigation & Design Institute Co., Ltd., Chengdu 610031, China; rengf0118@tom.com
- \* Correspondence: zhangxiaochao@cdut.cn (X.-C.Z.); peixj0119@tom.com (X.-J.P.)

**Abstract:** The experimental study on the water-holding characteristics of remolded loess was carried out, revealing the variation of water-holding characteristics with particle size composition and dry density. The results show that the air-entry value is positively correlated with the silt-sized content and negatively correlated with the sand-sized content. During the dehumidification of the specimens at a fixed dry density, when the air-entry value is between 9 and 10 Kpa, it is strongly influenced by the silt-sized content; however, beyond 10 Kpa, the sand-sized content is an important influencing factor. Changes in particle size composition have less influence on the residual water content. There is a non-linear relationship between the particle size composition and the slope  $\lambda$  of the dehumidification curve in the transition zone. Air-entry values, residual water content, saturated volumetric water content, and  $\lambda$  correlate well with dry density. Simulation tests were carried out using two power function models, including three variables. It was found that the VG model is a better fit than the Gardner model.

**Keywords:** remolded loess; soil–water characteristics curve; air-entry value; volumetric water content; particle size composition; dry density



**Citation:** Wang, X.-Q.; Zhang, X.-C.; Pei, X.-J.; Ren, G.-F. Effect of the Particle Size Composition and Dry Density on the Water Retention Characteristics of Remolded Loess. *Minerals* **2022**, *12*, 698. <https://doi.org/10.3390/min12060698>

Academic Editors: Qi Wang, Bei Jiang, Xuezhen Wu, Hongke Gao and Gianvito Scaringi

Received: 20 March 2022

Accepted: 23 May 2022

Published: 31 May 2022

**Publisher's Note:** MDPI stays neutral with regard to jurisdictional claims in published maps and institutional affiliations.



**Copyright:** © 2022 by the authors. Licensee MDPI, Basel, Switzerland. This article is an open access article distributed under the terms and conditions of the Creative Commons Attribution (CC BY) license (<https://creativecommons.org/licenses/by/4.0/>).

## 1. Introduction

Loess is loosening sediment formed during the Quaternary period and is yellowish-brown in color, with a predominantly silty composition. Loess and loess-like soils are widely distributed, covering an area of approximately 13 million km<sup>2</sup> worldwide, or 9.3% of the total global land area [1]. Many human engineering activities are carried out in loess areas. With the development of engineering technology, remolded loess is widely used as construction material, such as embankment fill, caves, dams, and other applications [2].

The shear strength and consolidation properties of soils are greatly influenced by the suction of the parent material in the soil [2]. At the same time, the parent material suction is directly related to the soil's water-holding capacity and is also very important for crop growth. Therefore, the study of the water retention properties of loess is a crucial point.

The soil–water characteristic curve can reflect different soils' water holding and releasing characteristics. It can be used to simulate the unsaturated permeability law [1–7], the shear strength of soil [8–10], the water migration in soil, the influence of water content change in soil on the mechanical properties, and the composition model of soil [11–17].

The main factors affecting the soil–water characteristic curve (SWCC) include mineral species and content of the soil, pore structure, particle size composition, stress history, and sample preparation method [18–23]. The change of compaction state of loess is very important for SWCC, as found by Zhang Xuedong et al. [19]. Wang Xiequn et al. [20] point out that the influence of compaction degree on SWCC of loess is mainly reflected in the

middle part of the curve. Vereecken et al. [21] show particle size composition is also an essential factor affecting the matric suction of soil. The research on the influence of particle size composition on soil water holding characteristics is mainly concentrated in clay and sand soil. Wen Baoping et al. [22] found particle size has a significant control effect on the soil–water characteristic curve. Li Zhuo et al. [16] show that with the increase in sand-sized content, the water holding capacity gradually decreases. Tian Hu et al. [23] indicate that after exceeding the air-entry value, the increase in silt-sized content significantly enhances the water holding capacity of sand. Zhao Yaqiong et al. [24] point out that the smaller the soil particle size, the more the medium and micropores pores and the worse the connectivity, according to Ku-PF measured soil–water characteristic curves of four soils with different particle compositions.

Regarding the water-holding capacity of remolded loess, current research has focused on factors such as water content and compactness, with less research conducted on particle size composition and a lack of quantitative analysis. As a construction material with different particle size compositions and dry densities, remolded loess has different basic physical and mechanical properties, and its soil–water characteristics curve is also different. It is necessary to carry out experimental studies on the water properties of loess with different particle size compositions and dry densities.

After measuring the matric suction, a series of measured matric suction and corresponding water content data need to be fitted and expressed as an equation to produce a soil–water characteristic curve (SWCC).

Commonly used are the Van Genuchten (1980) and Fredlund and Xing (1994) models [25]. Generally speaking, the more variables and the more complex the expression, the more accurate the fit. Therefore, the latter fits better than the former [26]. However, more variables can make it more challenging to use. To facilitate practical application in engineering and to ensure accuracy, the VG and Garden models with the same number of variables and similar complexity of mathematical expressions (both are three-variable equations with power functions for the mathematical expressions). Separate fits were carried out to verify the applicability to remodeled loess.

This paper used the soil–water characteristic curve (SWCC) test to summarize the water-holding characteristics of remolded loess with different particle size compositions and dry densities. By fitting the three-variable curve equation, the applicability of the remolded loess soil–water characteristic curve equation was analyzed, which provides a scientific reference for the prediction model of the soil–water characteristic curve.

## 2. Materials and Methods

### 2.1. Soil Samples

In China, projects such as the Yan'an New Area and Lanzhou's cutting of mountains to create a new city include dredging and filling work, upholding the principle of local extraction of materials, and remolded loess becoming a vital backfill material. Yan'an city infrastructure projects are carried out in large numbers; Yan'an new district, for example, the region has a large number of loess excavation and filling work, Malan loess is widely distributed, and large thickness is a common building material in filling engineering [25]. The test samples were collected from a newly excavated section of Nan Gou Village, Ansai District, Yan'an City, with a depth of 3 m below the surface of Malan loess. Figure 1 shows the geographical location of the sampling section. This sample made the remolded loess soil sample.

In order to better study the effect of particle size composition on water-holding characteristics of remolded loess, the particle size analysis of the collected samples was carried out to determine the contents of sand, silt, and clay. Figure 2 shows the particle size distribution of the samples by the MS-2000 particle size analyzer. Through indoor soil test [27], the basic physical properties of loess samples are measured, determination of water content by oven method, and determination of compaction degree by compaction test; the compaction curve is shown in Figure 3. The specific gravity is 2.7, the void ratio is 0.56, the liquid limit

is 30.6%, the plastic limit is 21.4%, and the plastic index is 9.2. Table 1 shows the essential physical properties of the sample.

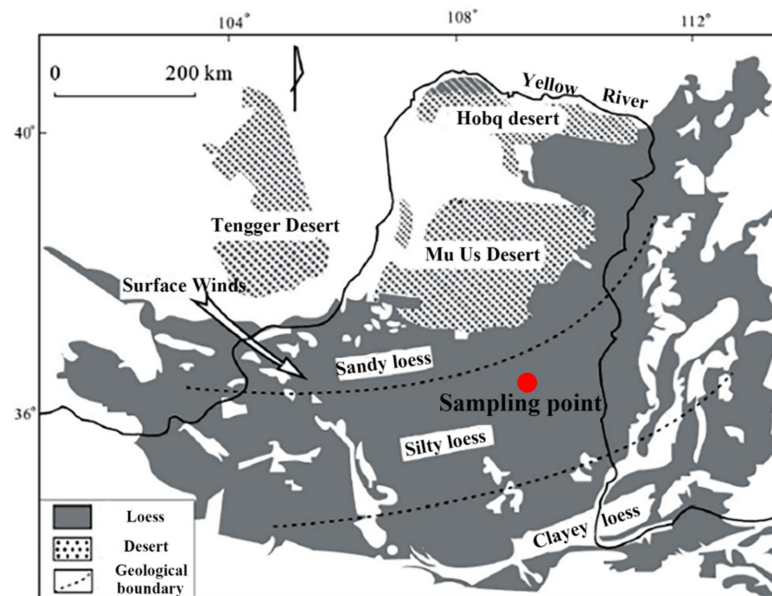


Figure 1. Geographical location of the sampling point.

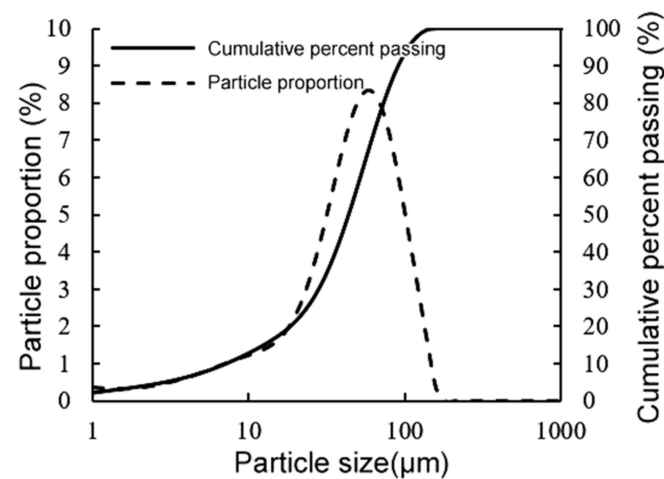


Figure 2. Particle size distribution of Yan'an Loess samples.

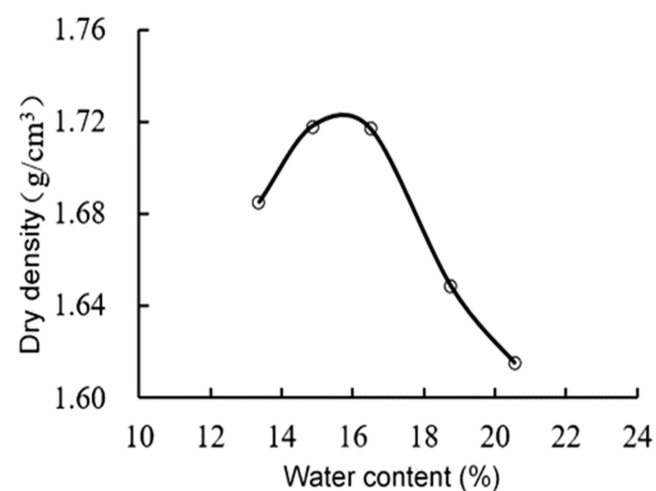


Figure 3. Compaction curve for the Yan'an loess.

**Table 1.** Basic physical properties of the loess samples.

Soil Description	Specific Gravity	Sand-Sized Particles	Silt-Size Particles	Clay-Sized Particles	Liquid Limit (w <sub>l</sub> )	Plastic Limit (w <sub>p</sub> )	Plastic Index (I <sub>p</sub> )	Void Ratio	Saturated Permeability Coefficient (K <sub>s</sub> ) or (m/s)
		0.075–2 mm	0.005–0.075 mm	<0.005 mm					
Yan'an loess	2.70	16.77%	76.68%	6.55%	30.6	21.4	9.2	0.56	1.26 × 10 <sup>-6</sup>

## 2.2. Test Equipment

Geotechnical sieve was used to prepare loess samples with coarse sieve aperture of 60, 40, 20, 10, 5, and 2 mm and 2.0, 1.0, 0.5, 0.25, and 0.075 mm. As shown in Figure 4a, a fine sieve was used as well.

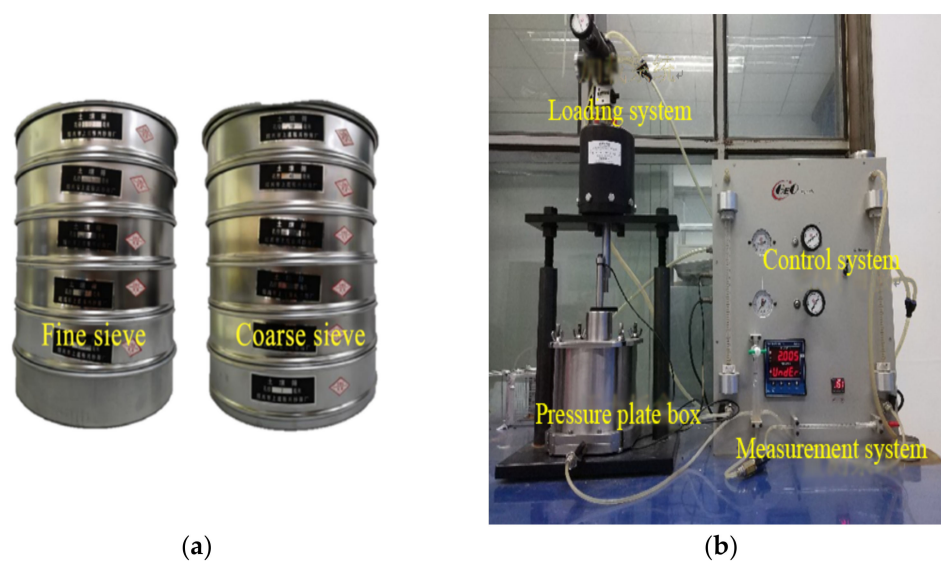


**Figure 4.** (a) Geotechnical sieve; (b) oedometer-type pressure plate SWCC apparatus.

The SWCC equipment (GEO-Experts) was used, as shown in Figure 4b. The apparatus mainly consists of four parts: loading, pressure plate box, control, and measurement system.

## 2.3. Sample Preparation

Particle size composition and dry density are important factors affecting the matric suction of soil [21]. To avoid the change of water-holding performance parameters caused by dry density, the first set of samples with dry density constant, the water-holding capacity of remolded loess, is studied only with different particle size compositions as variables.

The dry density  $\rho = 1.64 \text{ g/cm}^3$  corresponding to the compaction degree of the originally graded loess of 95% was taken as the reference target, denoted as S0. Five soil samples were prepared by mixing different particle compositions. The source of the sand particles was obtained by sieving the original loess to reveal the effect of different particle size compositions on the water-holding characteristics of the remolded loess. The specific methods are as follows:

The loess in the sampling area was screened by the screening method. The sand particles with particle sizes between 0.075 mm and 2 mm were selected to dry and mixed with fine-grained soil less than 0.075 mm after passing the minimum sieve hole to ensure that the content of sand particles was 10%, 20%, 30%, 60%, and 0% of the total mass. While keeping the dry density constant, five remolded loess samples were made, named S1, S2, S3, S4, and S5. After the remolded loess samples with different gradations were configured, the Mastersize2000 laser particle sizer was used to determine the actual particle content, and the results are shown in Figure 5.

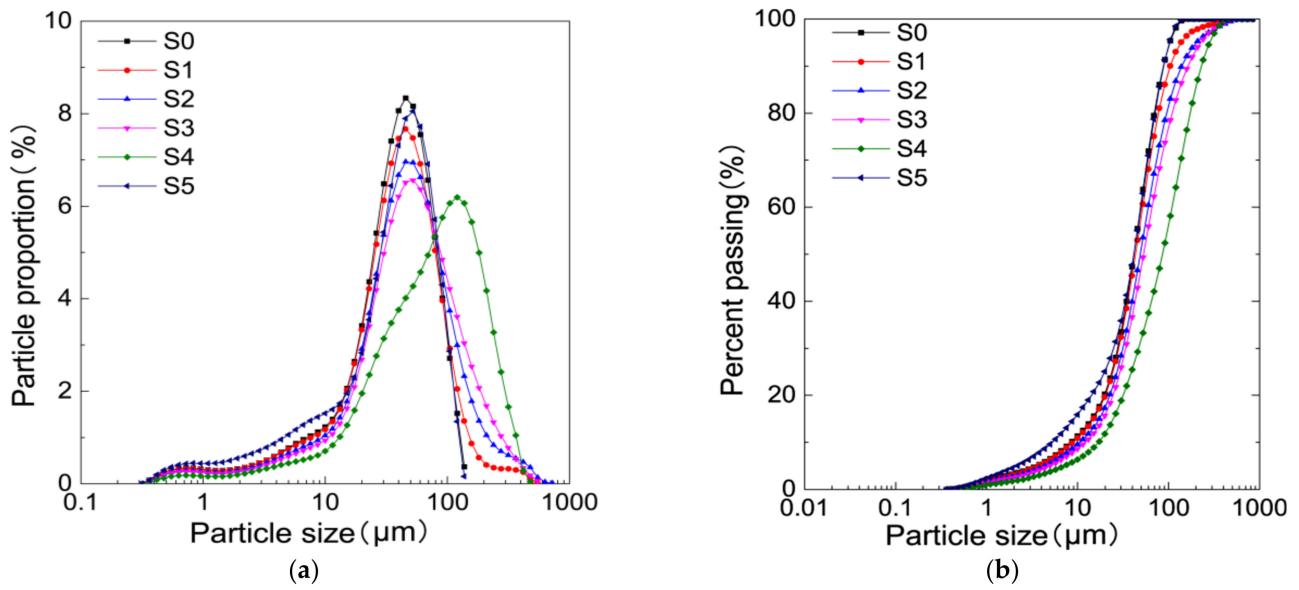


**Figure 5.** S0–S5 particle size characteristics of sample. (a) Particle size distribution curves of remolded loess samples; (b) cumulative particle size distribution curves of remolded loess samples.

In order to study the effect of dry density on water retention characteristics of remolded loess, another group of samples was made with the same particle size composition. Taking S0 as the reference target, two samples with different dry densities (1.56 and 1.38 g/cm<sup>3</sup>) were prepared. They are equivalent to 90% and 80% of the maximum dry density, respectively), and are designated as S6 and S7, respectively. Then S0, S6, and S7 are a set of samples with the same particle size and different dry densities.

Table 2 shows the results of C<sub>c</sub>, C<sub>u</sub>, and D<sub>10</sub>. C<sub>c</sub> is the curvature coefficient, C<sub>u</sub> is the inhomogeneity coefficient, and D<sub>10</sub> is the effective particle size.

The particle size distribution of the remolded samples was analyzed. Figures 5 and 6 show the resulting particle size distribution curves.

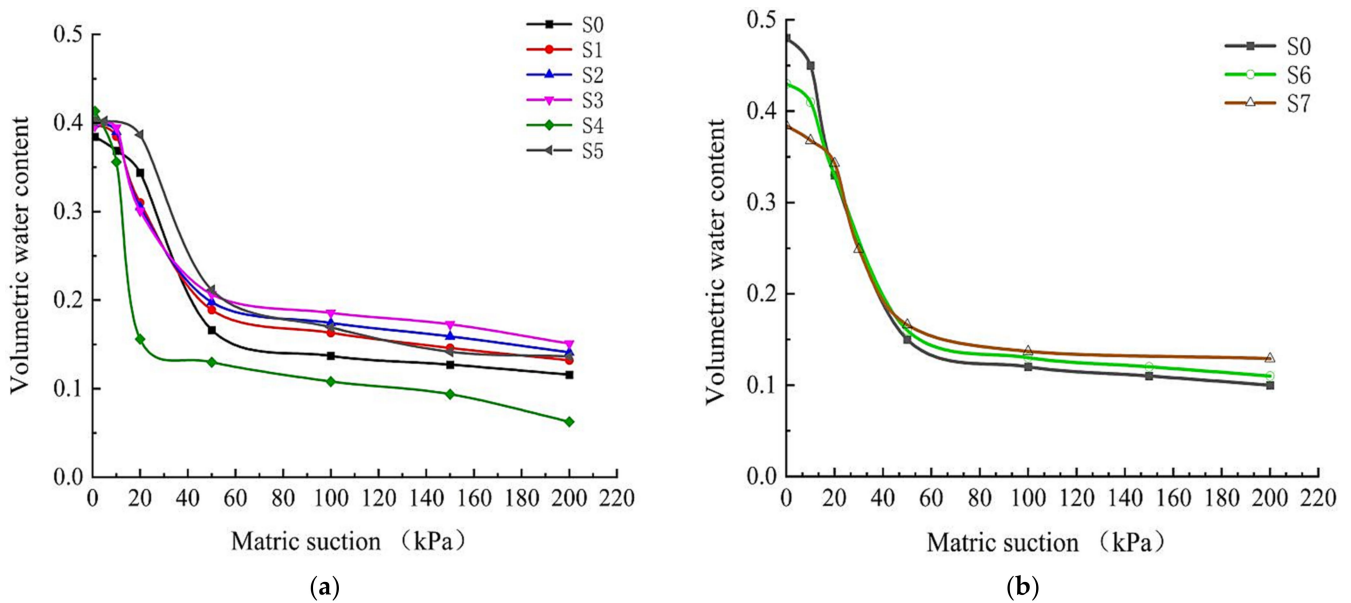


**Figure 6.** SWCC of loess samples. (a) Loess samples with different particle size compositions; (b) loess samples with different dry densities.

**Table 2.** SWCC testing scheme.

Id of the Samples	Dry Density (g/cm <sup>3</sup> )	Clay-Sized Content (%)	Silt-Sized Content (%)	Sand-Sized Content (%)	Cc	Cu	D10
S0	1.64	6.55	76.68	16.77	1.82	5.80	8.51
S1	1.64	6.39	72.1	21.51	1.75	5.86	8.86
S2	1.64	5.58	64.95	29.47	1.57	5.62	10.63
S3	1.64	5.07	60.61	34.32	1.44	5.45	12.11
S4	1.64	3.77	41.12	55.11	1.19	6.43	17.02
S5	1.64	9.6	79.56	10.84	2.35	9.44	5.29
S6	1.56	6.55	76.68	16.77	1.82	5.80	8.51
S7	1.38	6.55	76.68	16.77	1.82	5.80	8.51

### 3. Test Results and Analysis

#### 3.1. Test Results

Considering the different purposes of the remolded loess samples, the water retention parameters for SWCC are listed in Table 3. Figure 6 shows the SWCC of the remolded loess samples with different particle size compositions and dry densities.

**Table 3.** Water retention parameters for SWCC.

Parameters	S0	S1	S2	S3	S4	S5	S6	S7
Saturated volumetric water content (%)	38.4	39.8	39.9	39.6	41.3	40.2	43.3	48.2
Air-entry value (kPa)	14.0	10	9.1	10	8.2	17.1	10.6	9.1
Drying-cycle slope ( $\lambda$ )	4.63	3.84	3.53	4.04	6.69	5.05	4.66	4.71
Residual water content (%)	13.2	13.4	14.7	16.2	7.8	14.5	12	11
Residual matric suction (kPa)	54	79	78	55	24	61	56	60
Magnitude of water content variation (%)	25.2	26.4	25.2	23.4	33.5	25.7	31.3	37.2

#### 3.2. Analysis

The SWCC in Figure 6a shows differences in soil–water characteristic curves of loess soil samples with different particle size compositions. The volumetric water content decreases as the matric suction increases. In particular, for matric suctions in the range of 10–100 kPa, an increase in the matric suction leads to a marked decrease in the volumetric water content. However, for matric suctions above 100 kPa, the water content varies slightly and gradually approaches the residual water content. S5 residual moisture content is larger, soil–water characteristic curve relative to S0 overall right shift; S4 residual moisture content is small, soil–water characteristic curve relative to S0 overall left shift; S1, S2, and S3 showed a similar pattern. In particular, when the matric suction of S2 was greater than the air-entry value, the volumetric water content decreased rapidly, more significantly compared to S3. However, in the second half of the SWCC, for the first set of samples, S1, S2, and S3 had relatively good water retention capacity than those of S4 and S5, with a greater volumetric water content than sample S0. In addition, the remolded loess samples had bimodal SWCC. Specifically, the SWCC has two sharply decreasing sections, and the slope of the second section is smaller than that of the first section.

Figure 6b depicts the decrease in saturated volumetric water content with increasing dry density. In addition, the air-entry value increases with increasing dry density. According to the definition of dry density, the dry density is the ratio of the actual dry density to the maximum dry density. Therefore, as dry density increases, the soil particles tend to be closely packed, the pore volume decreases, and the space available for water retention in the soil is reduced. In particular, the SWCC has similar slope properties when the matric suction exceeds the air-entry value. The higher the dry density, the lower the infiltration coefficient, resulting in a lower variable rate of the SWCC. For the second half of the SWCC,

the higher the dry density, the higher the residual water content. In general, the SWCC with different dry densities samples shows only insignificant macro mass suction differences.

#### 4. Discussion

##### 4.1. Influence of Particle Size Composition on the Characteristic Values of the SWCC

It is known that the performance of SWCC is decisive on such factors as the air-entry value, residual water content, drying-cycle slope ( $\lambda$ ), sand-sized content, silt-sized content, and clay-sized content. To further investigate the correlation between these factors, the variation trend of the SWCC was simulated, and model regression analysis was carried out to find the relationship between different particle size compositions and water holding characteristics.

The air-entry value reflects the minimum matric suction when the soil begins to enter the unsaturated state from the saturated state. The test parameters are shown in Tables 2 and 3 (sample S0–S5).

All samples had a relatively low viscous particle content for the first set of data. The inlet values are not sensitive to changes in them. The sand-sized content and silt-sized content were defined as independent variables, and the variation of the air-entry value with both was sought; 1 stop software was used to fit a polynomial to the inlet air value, and particle content using the Levenberg–Marquardt method (LM) + Universal Global Optimization (UGO) algorithm, and the fitted model was subjected to regression analysis. A high level of significance of the correlation coefficient was ensured.

Defining the content of the sand-sized and silt-sized as  $x$  and  $y$ , both are the independent variables. Defining the air-entry value,  $z$  as the dependent variables, fitting using 1 stop software, the following Equation (3) was found.

$$z = p1 + p2 * \text{Exp}(-x) + p3/y^{1.5} \quad (1)$$

Correlation coefficient  $R = 0.971$  and  $\alpha = 0.05$ , where  $p1 = 11.09468$ ,  $p2 = 77,281,783$ , and  $p3 = 752.445$ .

In addition, clay-sized content is analyzed by a single factor correlation. The content of clay-sized content is defined as  $a$ , and the air-entry value is defined as  $b$ . It can be seen that the changing trend between the two variables is in the same direction, as shown in Figure 7d.

As shown in Figure 7a,b, the air-entry value is negatively correlated with the content of sand-sized content. The sand-sized content in the range of 15–20% has a noticeable control effect on air-entry value. When the sand-sized content is higher than 20%, the control effect is weakened. The air-entry value is positively correlated with the silt-sized content, especially when the silt-sized content is higher than 55%. As shown in the distribution range and slope of the curve Figure 7b, the silt-sized content dramatically influences the air-entry value in the range of air-entry value of 9–10 kPa. When the inlet value is higher than 10 kPa, the sand-sized content has a significant influence on the air-entry value. Figure 7c shows the spatial correlation between air-entry valve, sand-sized content, and silt-sized content. The single factor analysis shows that the content of clay-sized content is positively correlated with the air-entry valve, as shown in Figure 7d.

The matrix suction is closely related to the pore size. The smaller the pore radius, the greater the curvature of the curved surface and the greater the matrix suction [28]. It can be seen that the smaller the pore diameter is, the larger the intake value is. According to the grain relationship of loess, silt is the skeleton, and clay is adsorbed on the silt surface and locally exists in agglomerate [29]. Evidently, with the increase in clay particles, the invalid space occupied by cohesive surface water increases, the water storage space and effective seepage diameter of soil pores decrease, the permeability decreases, and the water-holding capacity increases. Therefore, the intake valve is positively correlated with the clay and silty content and negatively correlated with the sand content.

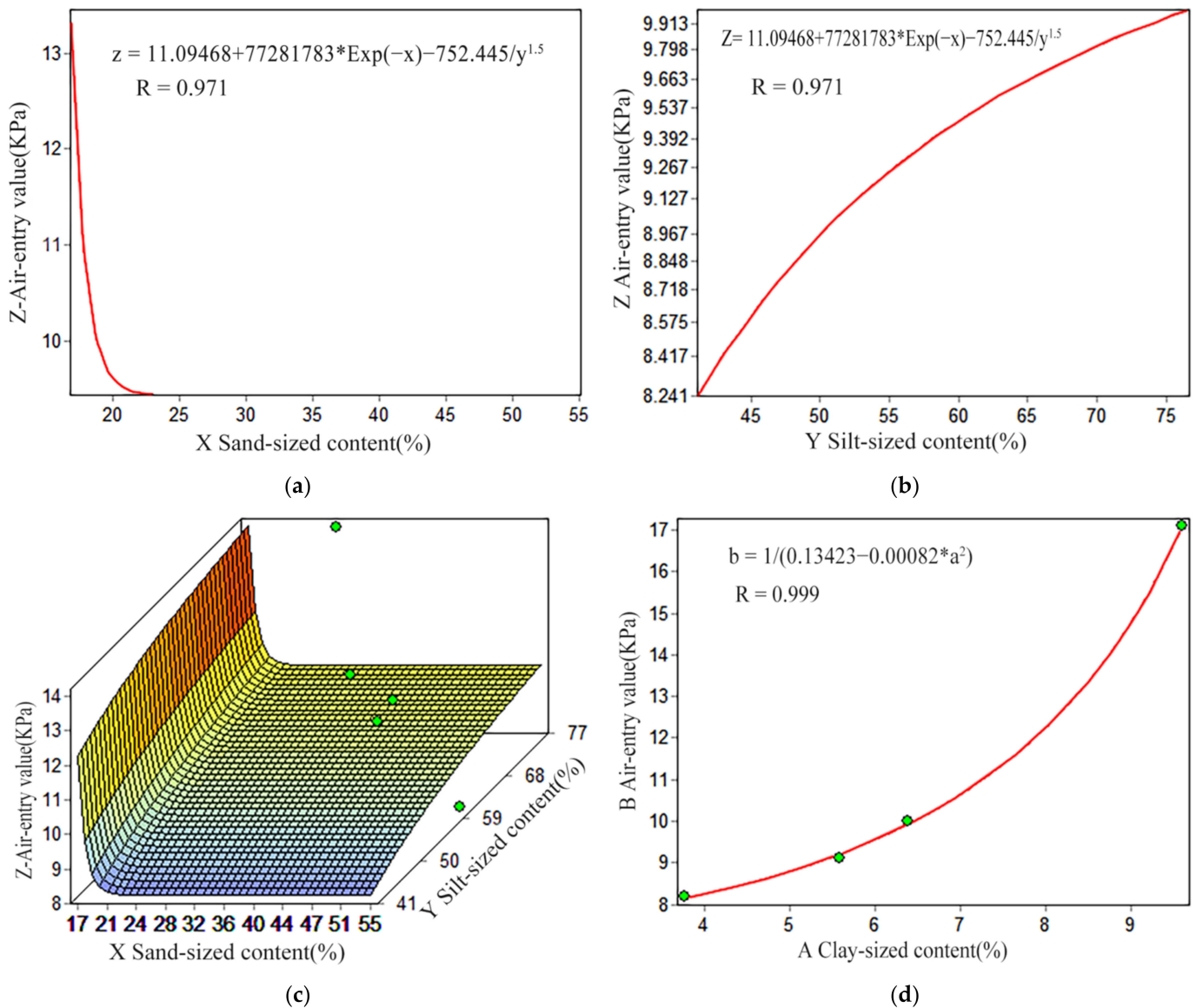


**Figure 7.** (a) Correlation between air-entry value and sand-sized content; (b) correlation between air-entry value and silt-sized content; (c) relationship between air-entry value and sand-sized and silt-sized content; (d) single-factor correlation between air-entry value and clay-sized content.

The water-holding capacity of soil is mainly controlled by the size of loess pores in a specific range. The pore distribution is often used to explain the macroscopic water-holding characteristics [30,31]. The conversion relationship of loess mechanical properties shows that the specific gravity of sand is smaller than that of silt and clay. Sample S0–S6 is a mixture of sand particles and fine particles. The larger the sand-sized content is, the smaller the specific gravity is, namely, the smaller the density of the solid pellet. The sample volume is the same. Under the condition of fixed dry density, the quality of solid pellet is the same; with the increase in solid pellet density, the void ratio increases. More conducive to capillary action of fine particles. Therefore, the smaller the sand-sized content, the stronger the capillary effect of fine particles, and the greater the air-entry value. With the increase in sand-sized content, the air-entry value decreases, and the water retention capacity decreases.

When we investigated the residual water content, we found that it did not vary significantly for different particle size compositions. The linear fit correlation was also not strong. The specific fits are shown in Figure 8.

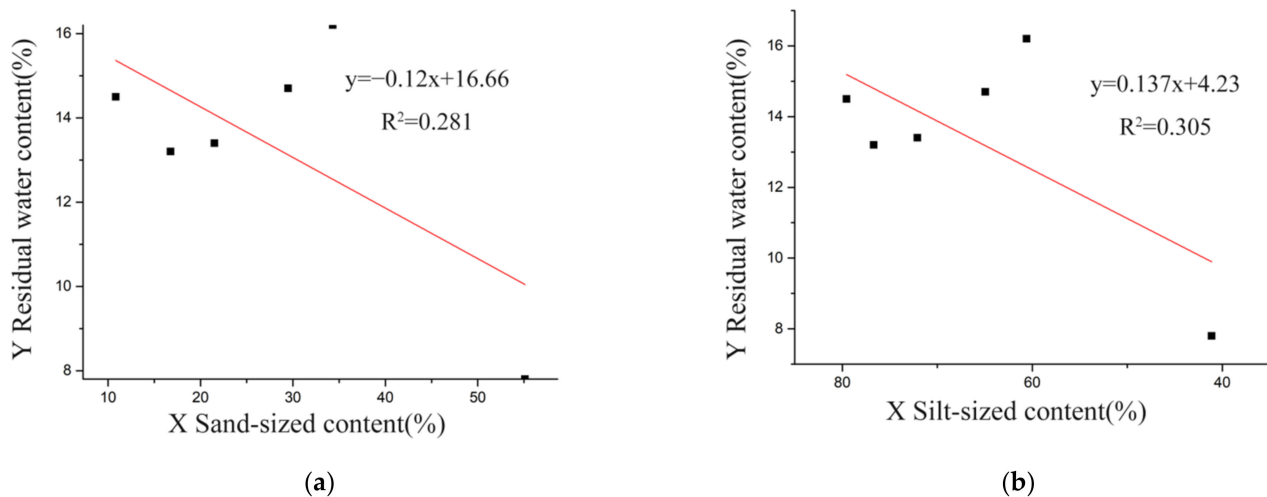


**Figure 8.** (a) Correlation between residual water content and sand-sized content; (b) correlation between residual water content and silt-sized content.

This is different from the research conclusion of Wen Baoping [22]. Wen believed that the residual water content of unsaturated soil had a significant positive linear correlation with clay-sized content and silt-sized content and also an excellent linear negative correlation with coarse grain content. This study analyzed the single-factor method's water-holding characteristics of remolded loess. Although the trend is the same as Wen Baoping's research results, it does not reflect a good linear relationship. The reason is that there is no fixed dry density value in Wen Baoping's test, and there is a situation in that dry density and particle size composition cross affect residual moisture content. The final residual moisture content is different from the results of this experiment. It is also possible that the coarse particles in the Wen Baoping experiment are breccia rather than sand. The particle size varies greatly, which changes the internal pore structure of the soil and obtains different changes. Further studies by Tian Hu et al. [23] have shown that in the residual moisture content part, the higher the silt-sized content and clay-sized content, the greater the corresponding moisture content. However, in the experimental data of Tian Hunan [23], the distribution of the residual water content is scattered, and the distribution pattern is not apparent. This is similar to the findings of this paper.

It can be seen that the influence of particle size composition on residual moisture content is weaker than that of the air-entry valve.

The correlation between the contents of sandy, silty, and clayey particles and the drying-cycle slope ( $\lambda$ ) was simulated for S1–S4. Figure 9 shows the resulting correlation curves. The correlation is nonlinear and satisfies the following equation:  $y = p_1 + p_2 * x + p_3 * x^2$ , ( $\alpha = 0.01$ ). The drying-cycle slope ( $\lambda$ ) is positively correlated with the content of sand-sized, as shown in Figure 9a. It is negatively correlated with the contents of silty and clayey particles, as shown in Figure 9b,c. All the three correlation curves reversed direction in the vicinity of S4. Research shows that when the residual water content is close to optimal, the drying-cycle slope ( $\lambda$ ) reaches the limit value. After that point, an increase in the content of fine particles can no longer lead to a decrease in  $\lambda$ .

#### 4.2. Influence of Dry Density on the Characteristic Values of the SWCC

To further investigate the correlation between SWCC parameters and dry density, analysis of the second set of sample data, the variation trend of the SWCC parameters was simulated and analyzed with respect to the contents of dry density.

The simulation parameters are shown in Tables 2 and 3 (S0, S6, and S7).

As shown in Figure 10, the characteristic values for the variation of the matrix suction are linearly correlated with the dry density. In particular, air-entry values and residual water content positively correlate with dry density. The correlation between air-entry values and dry density is robust. The saturated volumetric water content and the slope of

the drying cycle are negatively correlated with the dry density. The correlation between drying cycle slope and dry density is robust. The correlation between volumetric water content and drying cycle slope and dry density is stronger than for air-entry values and residual water content. This is mainly because, with the same particle size composition of the specimen, the higher the dry density, the greater the number of solid particles in the same volume and the tighter the arrangement, resulting in a lower pore ratio and a lower saturated volumetric water content. Within a certain range, the structural characteristics of the soil pores play a decisive role in the water-holding curve, and the pore distribution of the soil can be used to explain the variability of the water-holding properties [30]. A pore means less connectivity between the gaps, a stronger bond between the soil particles and the water film, greater water confinement between the pores, lower drainage rates, and more excellent water retention capacity. Therefore, soil samples with a more pronounced dry density have a smaller slope of the drying cycle and higher values of residual water content.

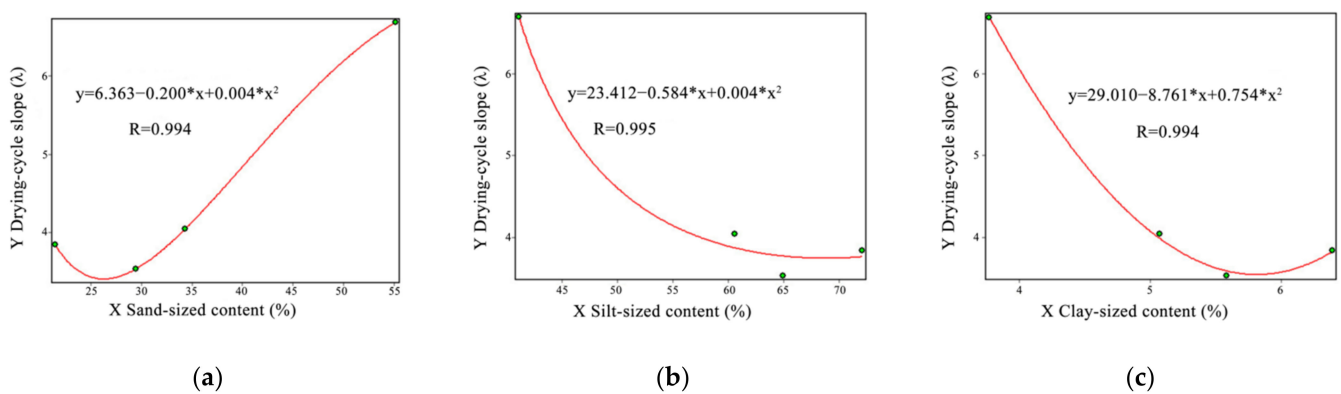


Figure 9. (a) Correlation between λ and sand-sized content; (b) correlation between λ and silt-sized content; (c) correlation between drying-cycle slope (λ) and clay-sized content.

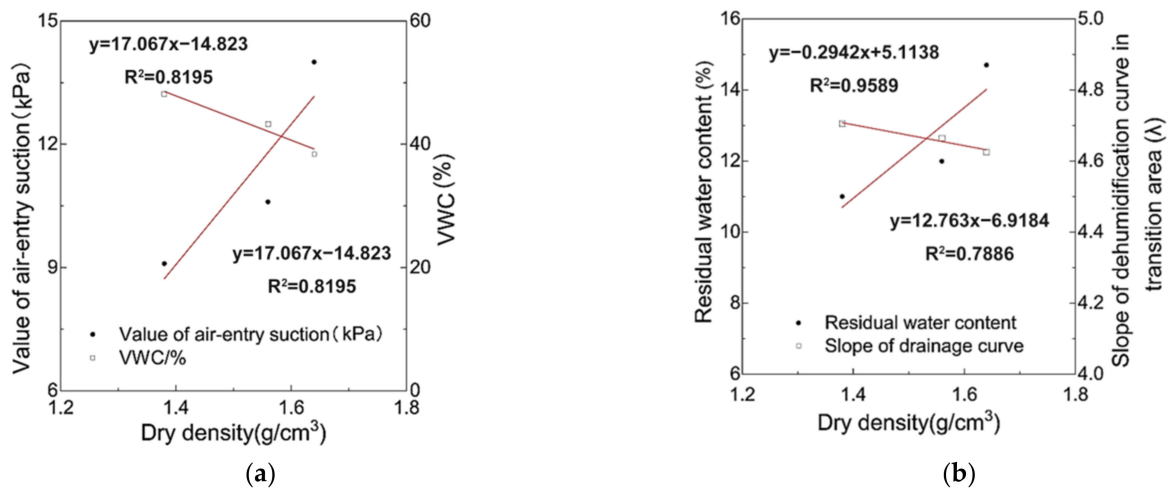


Figure 10. Correlation between SWCC parameters and dry density. (a) Relationship between value of air-entry suction, VWC and dry density. (b) Relationship between residual water content, λ and dry density.

### 4.3. Simulation of SWCC

In the application of the soil–water characteristic curve, the soil–water characteristic curve can be applied to the corresponding calculation only by turning the test scatter point into a continuous function. The commonly used soil–water characteristic curve (SWCC) equations are shown in Table 4. The equations describing the SWCC are complex and have many unknown parameters.

**Table 4.** Equation to express the soil–water characteristic curve [25].

Variable Category	Presented by	Expression Equation	Note Description
Dual variables	Farrel and Larson (1972)	$\theta = \theta_s - \frac{1}{\alpha_f} \ln \frac{\psi}{\psi_a}$	$\alpha_f$ is the fitting variable
	Williams J. (1983)	$\ln \psi = p + q \ln \theta$	$p, q$ are unknown fitting variables
	Chen Z. (1993)	$S_r = b - \text{clg}\left(\frac{\psi}{p_{atm}}\right)$	$b$ and $c$ are the fitted variables related to the dry density or porosity of the soil
Three variables	Gardner (1958)	$\theta = \theta_r + \frac{\theta_s - \theta_r}{1 + (\psi/a)^n}$	$a$ is the variable related to the inlet value, $n$ is the variable related to the slope of the curve when $\psi > \psi_a$
	Brooks and Corey (1964)	$\Theta = 1$ for $\psi \leq \psi_a$ $\Theta = \left[\frac{\psi_a}{\psi}\right]^\lambda$ for $\psi > \psi_a$	$\lambda$ is the aperture parameter
	Van Genuchten and Burdine (1980)	$\Theta = \frac{1}{[1 + (\psi/a)^n]^{(1-\frac{2}{n})}}$	
	Van Genuchten and M ualem (1980)	$\Theta = \frac{1}{[1 + (\psi/a)^{b_m}]^{(1-\frac{1}{b_m})}}$	$b_m$ is the soil variable that controls the SWCC
	Fredlund and Xing (1994)	$\theta = \frac{\theta_s}{\{\ln[e + (\psi/a)^n]\}^m}$	$m$ is the variable related to the residual moisture content
Four variables	Fredlund and Xing (1994)	$\theta = C(\psi) \frac{\theta_s}{\{\ln[e + (\psi/a)^n]\}^m}$ $C(\psi) = 1 - \frac{\ln(1 + \psi/\psi_r)}{\ln[1 + (10^6/\psi_r)]}$	
	Van Genuchten (1980)	$\Theta = \frac{1}{[1 + (\psi/a)^n]^m}$	

Soil–water characteristic curve equation, according to the mathematical form [26], can be divided into the form of power function of logarithmic function expression of the mathematical model. The mathematical model is in the form of the power function. Fractal model of the soil–water characteristic curve. The mathematical model is in logarithmic function form. Many scholars compare the three-parameter equation with the four-parameter equation and find that the four-parameter equation is better than the three-parameter equation [25]. This comparison has little practical significance. Under the same assumptions, because the more parameters are, the more complex the mathematical expression of the equation is and the higher the accuracy is, which is expected. Therefore, when fitting the soil–water characteristic curve, the equation with equal parameters and similar mathematical expressions should be selected, with greater practical significance and comparison. Considering complex equations and more parameters will make the equation more complicated. In order to facilitate the practical application of engineering, under the premise that the number of unknown parameters is the same and the complexity of the mathematical expression of the equation is similar, this paper uses MATLAB software to fit the Gardner model and Van Genuchten model with the same mathematical expression as the power function and three parameters according to the test results.

(1) Gardner equation:

$$\theta_w = \theta_r + \frac{\theta_s - \theta_r}{1 + \left(\frac{\psi}{\alpha}\right)^n} \tag{2}$$

where  $\theta_w$  is the volumetric water content (%),  $\theta_s$  is the saturated volumetric water content (%),  $\theta_r$  is the residual volumetric water content (%),  $\psi$  is the matric suction (kPa),  $\alpha$  is the parameter related to the air-entry value (kPa), and  $n$  is the parameter related to the water drainage rate after the matric suction exceeds the air-entry value.

(2) Van Genuchten equation:

$$\theta_w = \theta_r + \frac{\theta_s - \theta_r}{[1 + (\alpha \cdot \psi)^n]^{(1-\frac{1}{n})}} \tag{3}$$

Equation (3) parameters are the same as those in Equation (2).

Figures 11 and 12 show the experimental data and the SWCC simulated using the two models. Table 4 shows the SWCC simulation parameters.

As shown in Table 5, the VG equation has better goodness of fit than the Gardner equation. The simulated SWCC for S0, S1, and S2 have small SSR and good goodness of fit. The simulated SWCC for S3, S4, and S5 have relatively large SSR. The simulated SWCC for the loess samples with different dry densities have small SSR and show good goodness of fit. It suggests that the loess in the sampling area is more suitable for using the VG model.

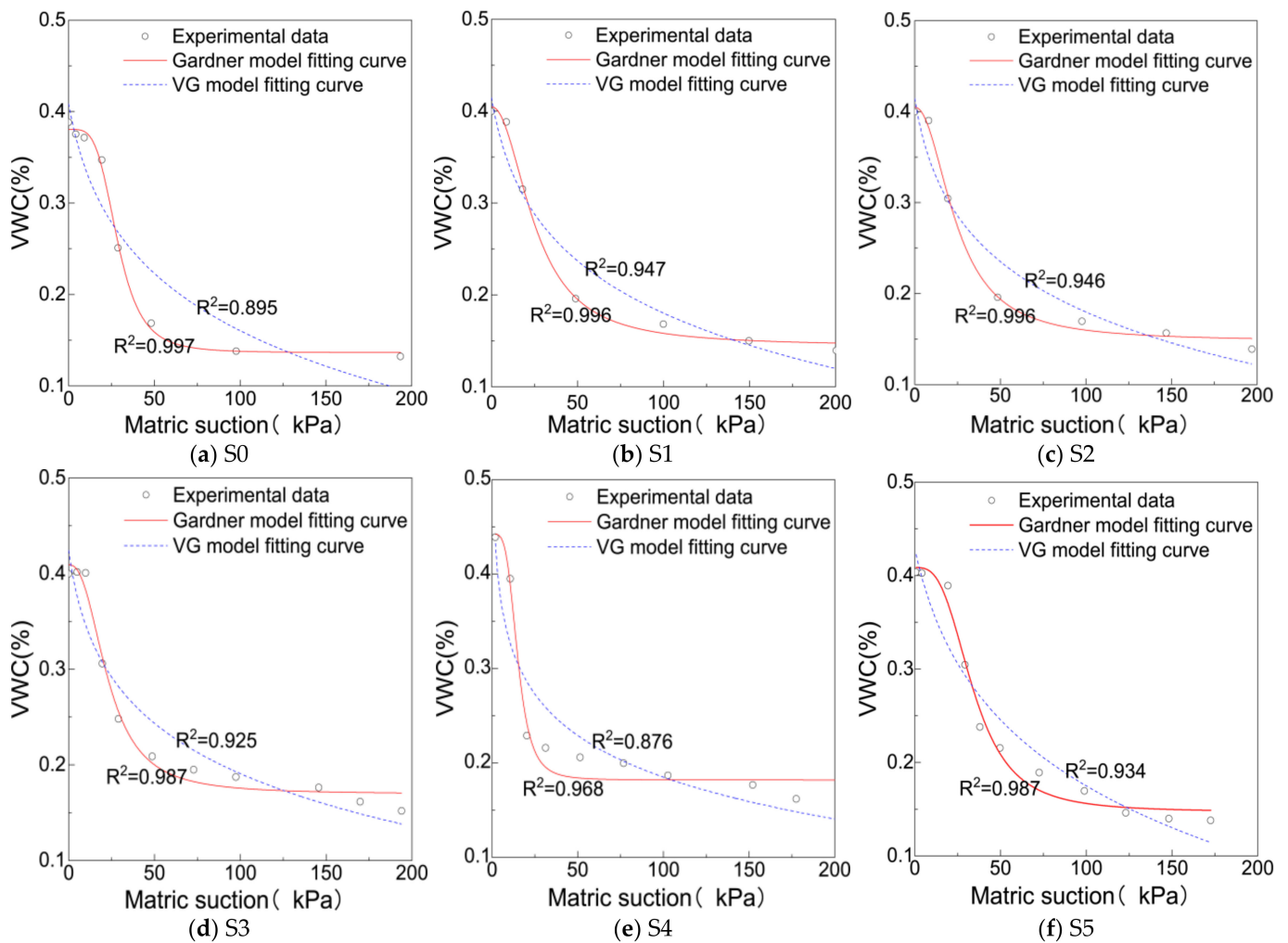


**Figure 11.** Experimental data and simulated SWCC of loess samples with different particle size compositions.

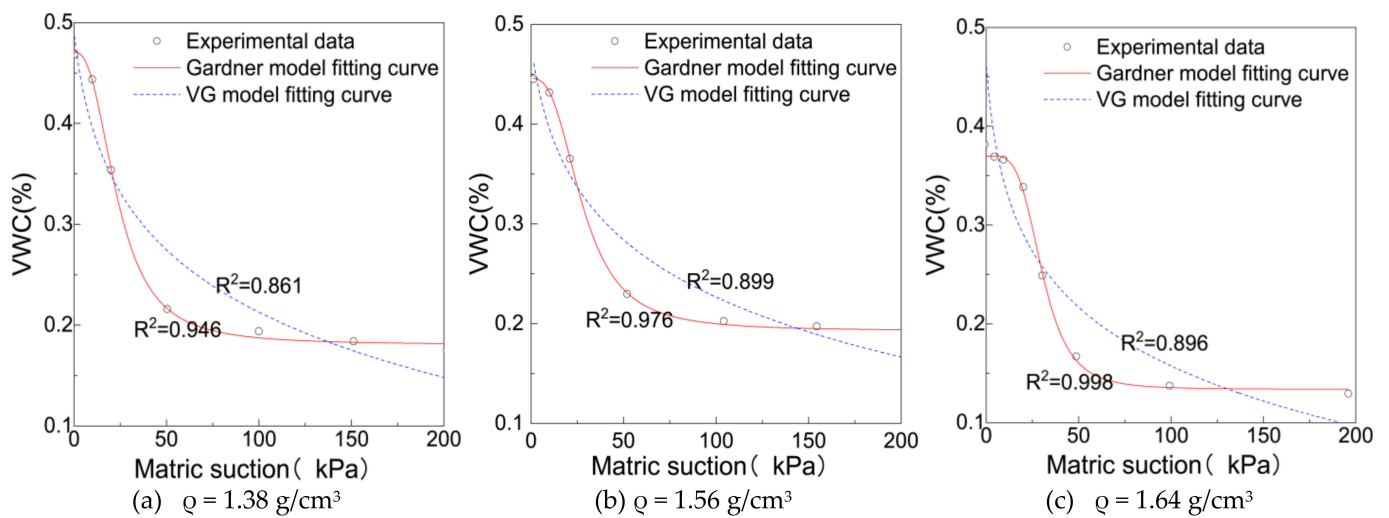


Figure 12. Experimental data and simulated SWCC of loess samples with different dry densities.

Table 5. SWCC parameter simulation and accuracy test ( $\alpha = 0.05$ ).

Id of Samples	Simulation Model	<i>a</i>	<i>n</i>	$\theta_s$	$\theta_r$	Sum of Squares of Residues (SSR)
S0	Van Genuchten	0.036	4.408	0.376	0.132	$1.876 \times 10^{-4}$
	Gardner	0.033	4.010	0.377	0.133	$2.289 \times 10^{-4}$
S1	Van Genuchten	0.049	2.661	0.402	0.134	$2.185 \times 10^{-4}$
	Gardner	0.037	2.295	0.402	0.140	$3.178 \times 10^{-4}$
S2	Van Genuchten	0.051	2.664	0.405	0.147	$3.957 \times 10^{-4}$
	Gardner	0.039	2.287	0.406	0.152	$5.461 \times 10^{-4}$
S3	Van Genuchten	0.054	2.764	0.403	0.162	$9.254 \times 10^{-4}$
	Gardner	0.043	2.415	0.404	0.167	$1.195 \times 10^{-3}$
S4	Van Genuchten	0.079	3.847	0.417	0.097	$3.542 \times 10^{-3}$
	Gardner	0.070	3.608	0.417	0.099	$3.804 \times 10^{-3}$
S5	Van Genuchten	0.033	3.598	0.406	0.145	$1.054 \times 10^{-3}$
	Gardner	0.029	3.269	0.407	0.148	$1.283 \times 10^{-3}$
S6	VG	0.046	3.180	0.429	0.113	$8.271 \times 10^{-3}$
	Gardner	0.038	2.7408	0.430	0.116	$9.544 \times 10^{-3}$
S7	VG	0.052	3.100	0.480	0.103	$6.874 \times 10^{-3}$
	Gardner	0.043	2.668	0.482	0.106	$1.160 \times 10^{-4}$

5. Conclusions

By analyzing the effect of particle size composition and dry density on SWCC of remolded loess, the results can be summarized as follows:

- (1) The air-entry value is sensitive to particle size composition and dry density change. The effect of particle size composition on residual water content is weak. With the increase in matric suction, the influence of dry density on the soil–water characteristic curve gradually weakened. In particular, dry density no longer affects indigenous water characteristic curves when the matric suction increases to more than 100 Kpa.
- (2) When the dry density remains constant, the unsaturated air-entry value is positively correlated with clay-sized content and silt-sized content, while it is negatively correlated with sand-sized content. In the particles, when the air-entry valve is in the

range of 9–10 kPa, the powder content greatly influences the intake valve. When the intake value is higher than 10 kPa, the content of sand significantly influences the intake value.

- (3) When the dry density remains constant, the correlation between the content of sand-sized, silt-sized, clay-sized, and the drying period slope ( $\lambda$ ) is non-linear and satisfies the following formula:  $Y = P1 + P2 * X + P3 * X^2$ . When the residual water content is near the optimum,  $\lambda$  reaches the limit value.
- (4) The experimental data obtained using different dry density samples show that air-entry value and residual water content are positively correlated with dry density. On the contrary, saturated volume water content and drying cycle slope were negatively correlated with dry density.
- (5) The Gardner and Van Genuchten models are selected as they are both power functions containing three variables, fitted to the measured data, and the VG model was found to be more accurate in fitting the model to the reshaped loess water–soil characteristic curve.

The above research provides theoretical support for slope erosion, geological disaster control, and soil conservation in the sampled area. It also provides a scientific basis for establishing and optimizing the characteristic curve prediction model in this area.

**Author Contributions:** Conceptualization, X.-Q.W. and X.-C.Z.; methodology, X.-Q.W.; software, G.-F.R.; validation, X.-J.P., G.-F.R. and X.-C.Z.; formal analysis, X.-Q.W. and G.-F.R.; investigation, X.-C.Z.; resources, X.-Q.W.; data curation, X.-J.P.; writing—original draft preparation, X.-Q.W.; writing—review and editing, X.-Q.W.; visualization, X.-C.Z.; supervision, X.-J.P.; project administration, X.-J.P. All authors have read and agreed to the published version of the manuscript.

**Funding:** This project was partially supported by the Major Program of the National Natural Science Foundation of China (grant no. 41790445) Source: NSFC, amount: 3.3 million yuan.

**Data Availability Statement:** The authors confirm that the data supporting the findings of this study are available within the article.

**Acknowledgments:** The authors particularly appreciate the valuable comments made by the editors and reviewers to make a substantial improvement to this manuscript.

**Conflicts of Interest:** The authors declare no conflict of interest.

## References

1. Liu, D. *Loess and Environment*; Science Press: Shanghai, China, 1985.
2. Hu, Z.; Lu, Z.; Yao, H.L. The water retention characteristics of an unsaturated compacted loess material. *Key Eng. Mater.* **2016**, *703*, 396–399. [[CrossRef](#)]
3. *D5298-10*; Standard Test Method for Measurement of Soil Potential (Suction) Using Filter Paper. ASTM International: West Conshohocken, PA, USA, 2013.
4. Zhang, X.; Zhong, Y.; Pei, X.; Duan, Y. A Cross-Linked Polymer Soil Stafor Hillslope Conservation on the Loess Plateau. *Front. Earth Sci.* **2021**, *955*, 771316. [[CrossRef](#)]
5. Chen, Y.; Uchimura, T. Influence of particle size on water retention of soils. *Chin. J. Rock Mech. Eng.* **2016**, *35*, 1474–1482.
6. Li, M.; Zhang, X.; Yang, Z.; Yang, T.; Pei, X. The rainfall erosion mechanism of high and steep slopes in loesslands based on experimental methods and optimized control measures. *Bull. Eng. Geol. Environ.* **2020**, *79*, 4671–4681. [[CrossRef](#)]
7. Fan, S.; Zhang, X.; Pei, X. Experimental study on soil-water characteristic curve of undisturbed loess in different regions and its application to slope stability evaluation. *Water Resour. Hydropower Eng.* **2019**, *50*, 154–161.
8. Gallage, C.; Kodikara, J.; Uchimura, T. Laboratory measurement of hydraulic conductivity functions of Two unsaturated sandy soils during drying and wetting processes. *Soils Found.* **2013**, *53*, 417–430. [[CrossRef](#)]
9. Pei, X.; Zhang, X.; Guo, B.; Wang, G.; Zhang, F. Experimental case study of seismically induced loess liquefaction and landslide. *Eng. Geol.* **2017**, *223*, 23–30. [[CrossRef](#)]
10. Hu, R.; Chen, Y.; Zhou, C. A water retention curve model for deformable soils based on pore size distribution. *Chin. J. Geotech. Eng.* **2013**, *35*, 1451–1462.
11. Kong, L.; Sayem, H.; Tian, H. Influence of drying-wetting cycles on soil-water characteristic curve of undisturbed granite residual soils and microstructure mechanism by nuclear magnetic resonance (NMR) spin-spin relaxation time (T2) relaxometry. *Can. Geotech. J.* **2018**, *55*, 208–216. [[CrossRef](#)]

12. Zhang, S.; Zhang, X.; Pei, X.; Wang, S.; Huang, R.; Xu, Q.; Wang, Z. Model test study on the hydrological mechanisms and early warning thresholds for loess fill slope failure induced by rainfall. *Eng. Geol.* **2019**, *258*, 105135. [[CrossRef](#)]
13. Li, P.; Li, T.L.; Wang, H.; Liang, Y. Predicting the soil-water characteristic curve and permeability coefficient of unsaturated loess using the Childs & Collis-Geroge model. *Rock Soil Mech.* **2013**, *34*, 184–189.
14. Zhang, X.; Pei, X.; Zhang, Z.; Song, L. Study on pore pressure and fluidization evaluation method of unsaturated loess in vibration process. *Bull. Eng. Geol. Environ.* **2021**, *80*, 5575–5587. [[CrossRef](#)]
15. Li, X.; Li, J.H.; Zhang, L.M. Predicting bimodal soil-water characteristic curves and permeability functions using physically-based parameters. *Comput. Geotech.* **2014**, *57*, 85–96. [[CrossRef](#)]
16. Li, Z.; Feng, H.; Wu, P.T.; Zhao, X.N.; Guo, Z. Simulated experiment on effects of soil clay particle content on soil water holding capacity. *J. Soil Water Conserv.* **2009**, *23*, 204–208.
17. Malaya, C.; Sreedeeep, S. Critical review on the parameters influencing soil-water characteristic curve. *J. Irrig. Drain.* **2012**, *138*, 55–62. [[CrossRef](#)]
18. Nam, S.; Gutierrez, M.; Diplas, P.; Petrie, J.; Wayllace, A.; Lu, N.; Muñoz, J.J. Comparison of testing techniques and models for establishing the SWCC of riverbank soils. *Eng. Geol.* **2009**, *110*, 1–10. [[CrossRef](#)]
19. Zhang, X.; Zhao, C.; Cai, G. Influence of soil density on soil-water characteristic curve. *Rock Soil Mech.* **2010**, *31*, 1463–1468.
20. Wang, X.; Zou, W.; Luo, Y. Influence of degree of compaction and gradation on soil-water characteristic curve of remolded clay in subgrade. *Geomechanics* **2011**, *32*, 181–184.
21. Vereecken, H.; Maes, J.; Feyen, J.; Darius, P. Estimating the soil moisture retention characteristic from texture, bulk density, and carbon content. *Soil Sci.* **1989**, *148*, 389–403. [[CrossRef](#)]
22. Wen, B.; Hu, Y. Effect of particle size distribution on the matric suction of unsaturated clayey soils. *Hydrogeol. Eng. Geol.* **2008**, *35*, 50–55.
23. Tian, H.; Kong, L. Experimental study on the effect of fine particles on the water retention capacity of sandy soil. *Rock Soil Mech.* **2010**, *31*, 56–60.
24. Zhao, Y.; Wang, Z.; Wang, W.; Chen, L.; Zhang, Z. Determination and simulation modelling of the soil-water characteristic curve at different particle sizes. *China Sci. Pap.* **2015**, *10*, 287–290.
25. Fan, J. The Study on Soil Water Characteristic Curve and Permeability Curve of Unsaturated Remolded Loess under Different Dry Density. 2020. Available online: [https://kns.cnki.net/kcms/detail/detail.aspx?dbcode=CMFD&dbname=CMFD202101&filename=1021567776.nh&uniplatform=NZKPT&v=183fcRXH9NmI3pWEhrLGgw\\_bCyirgtZfanAlmLbAK9wpR67m5hmbIR5Csywe7hbJ](https://kns.cnki.net/kcms/detail/detail.aspx?dbcode=CMFD&dbname=CMFD202101&filename=1021567776.nh&uniplatform=NZKPT&v=183fcRXH9NmI3pWEhrLGgw_bCyirgtZfanAlmLbAK9wpR67m5hmbIR5Csywe7hbJ) (accessed on 2 May 2022).
26. Qi, G.; Huang, R. Study on general mathematical model of soil-water characteristic curve. *J. Eng. Geol.* **2004**, *12*, 182–186.
27. *JTG 3430-2020; Test Methods of Soils for Highway Engineering*. Ministry of Transport: Beijing, China, 2020.
28. Xiong, C.; Liu, B.; Zhang, J. Relation of matric suction with moisture state density state of remolded cohesive soil. *Chin. J. Rock Mech. Eng.* **2005**, *24*, 321–327.
29. Yan, Y.; Wen, B. Relationship between Matric Suction Characteristics and Physical Properties of Unsaturated Remolded Loess. *Hydrogeol. Eng. Geol.* **2011**, *38*, 49–56.
30. Fredlund, D.G.; Xing, A. Equations for the soil-water characteristic curve. *Can. Geotech. J.* **1994**, *31*, 521–532. [[CrossRef](#)]
31. Niu, G.; Sun, D.A.; Shao, L.; Zeng, L. Water retention curve of complete-intense weathering mudstone and its estimation from pore-size distribution. *Rock Soil Mech.* **2018**, *39*, 1337–1345.